VII. Network Development and Operations

A. High-Rate Telemetry Project, *R. C. Tausworthe*

The following articles report the progress of the high-rate telemetry (HRT) project.[1] The test set configuration is described, some changes to the correlator design are given, the latest updates to the software are discussed, actual measured performance of the entire system in the compatibility test area is shown, and the effects of variation in subcarrier loop parameters on the subcarrier demodulator performance are described.

There have been no alterations in the project schedule. Field set I is en route to Cape Kennedy DSS to be installed and checked out for prelaunch spacecraft support. Field set II is in operation in the compatibility test area, giving performance identical to its predecessor. Laboratory set A is being updated to be the electrical equivalent of the two field sets.

B. Test Equipment, *R. I. Greenberg*

1. Physical Configuration

Figure 1 shows the final front panel configuration of the test equipment. The subassemblies are positioned from top to bottom as follows:

(1) Power supply.

(2) Control.

(3) Code generator.

(4) Frequency counter.

A fan located at the top is provided to cool equipment within the cabinet.

2. Controls

a. Power supply subassembly.

Voltage readout meter and voltage selector switch. The selector switch on the left may be positioned to choose any of the following four voltages for readout: ± 12 V ± 15 V. Normal reading will be "100," corresponding to the nominal voltage.

Marginal voltage control. The choice of marginal check voltages (± 12 V) in all possible combinations may be made by the selector switch on the right. The marginal voltages are provided to check the logic circuitry of the code generator during preventive maintenance in order to anticipate faulty operation. The lever switch, located below the selector switch, overrides all positions of the selector switch. In the normal position, nominal ± 12 V only are available.

b. Control subassembly.

The noisy channel selector switch. When the noise generator and signal/noise mixer are properly connected, the

[1]Previous reporting on this project is given in SPS 37-48, Vol. II, pp. 83–130, SPS 37-49, Vol. II, pp. 115–127, SPS 37-51, Vol. II, pp. 127–157, and SPS 37-52, Vol. II, pp. 141–143.

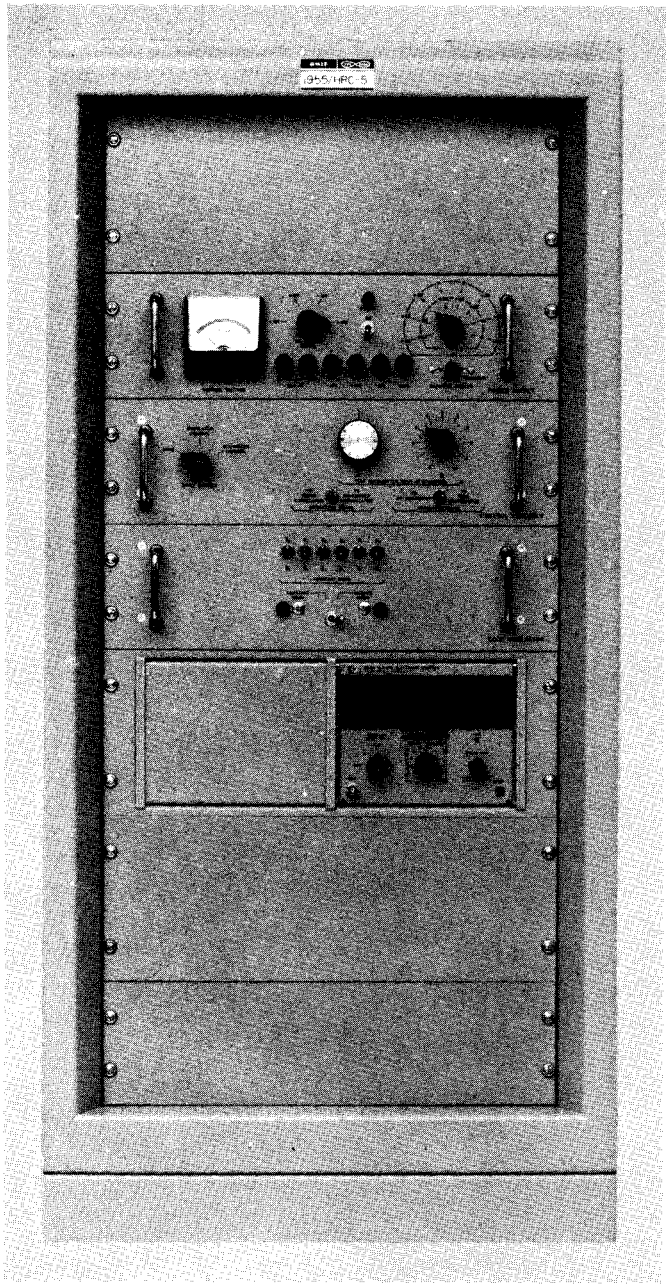

Fig. 1. Front panel of test equipment

selection of the noisy channel may be made by this switch. Note that only one channel may be chosen for noise addition. The other channel will be without noise.

Selection of outputs. This may be done by the two toggle switches located at the lower right. The left switch permits choice of outputs either to the cross correlator or to the subcarrier demodulator. The right switch permits choice of output either to the up converter or to the test transmitter. Note that the choice of output by either switch does not affect the choice of output of the other switch.

Attenuators. The variable attenuators, located above the toggle switches, apply only to the test transmitter output. The other outputs are fixed.

c. Code generator subassembly. Two modes of operation are possible for the code generator subassembly.

Mode choice toggle switch. Either random word output or constant word output may be chosen by this switch, which is located at bottom center.

Constant word choice switches. This constitutes a grouping of six toggle switches, which provide the capability of choosing any one of 64 words for the output.

3. Outputs

All outputs are clearly marked with connector numbers and function description at the rear panels of the subassemblies. The outputs are:

(1) To cross correlator from control subassembly.

(2) To subcarrier demodulator from control subassembly.

(3) To up converter from control subassembly.

(4) To test transmitter from control subassembly.

(5) Word sync from code generator subassembly.

(6) Symbol sync from code generator subassembly.

Outputs listed (1) through (4) must be terminated by 50 Ω to obtain the output voltages required. Termination requirements for (5) and (6) are unspecified.

4. Performance

The field units and the laboratory unit have been in operation for several months. Some difficulties were initially present, but these were corrected. Since then, the test equipment has been functioning without any apparent problems.

C. Digital Equipment, *H. C. Wilck*

1. Design Changes

Figure 2 shows a block diagram of the digital equipment. The 10-bit digital-to-analog (D/A) converter,

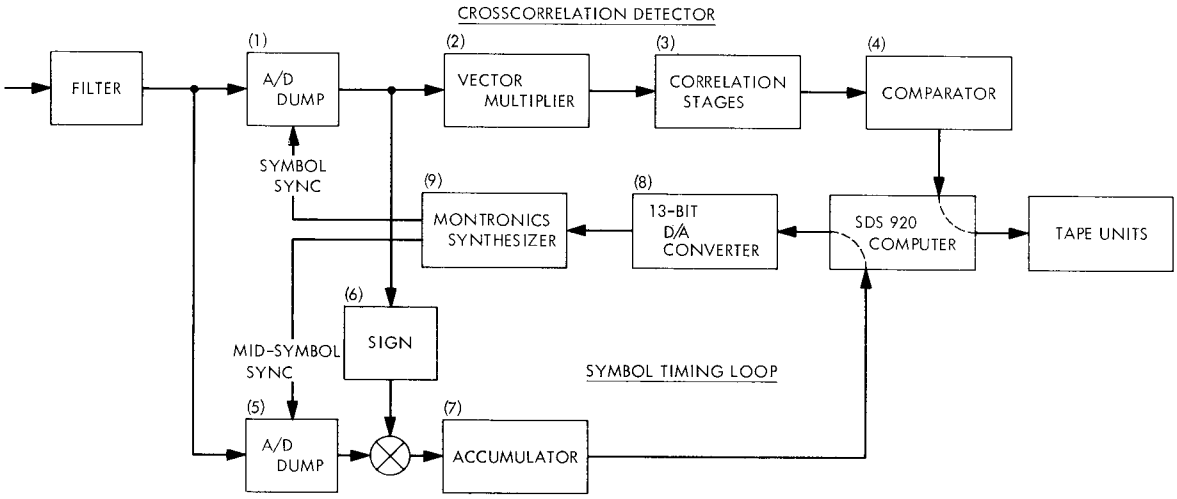

Fig. 2. Digital equipment diagram

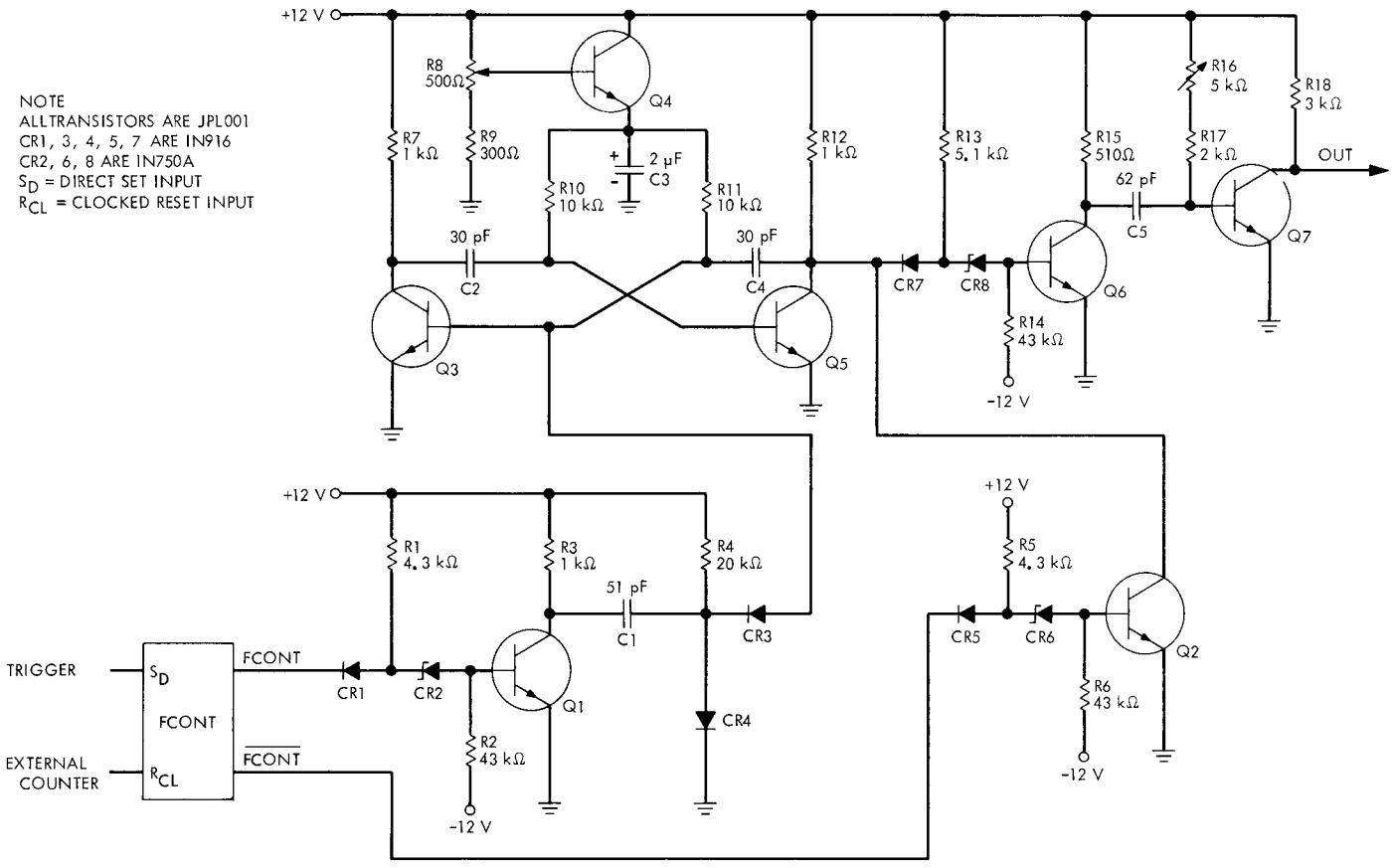

Fig. 3. Clock generator schematic

block (8) of Fig. 2, was changed to 13 bits. Also, the Hewlett–Packard frequency synthesizer, block (9) of Fig. 2, was replaced by a Montronics Model 314B-5; the Montronics synthesizer is capable of searching symmetrically around any frequency within its range, while the Hewlett–Packard searches over full decades only. Both the D/A change and the synthesizer change improve the voltage-controlled oscillator resolution in the symbol loop, and this in turn allows the loop to operate at a narrower bandwidth.

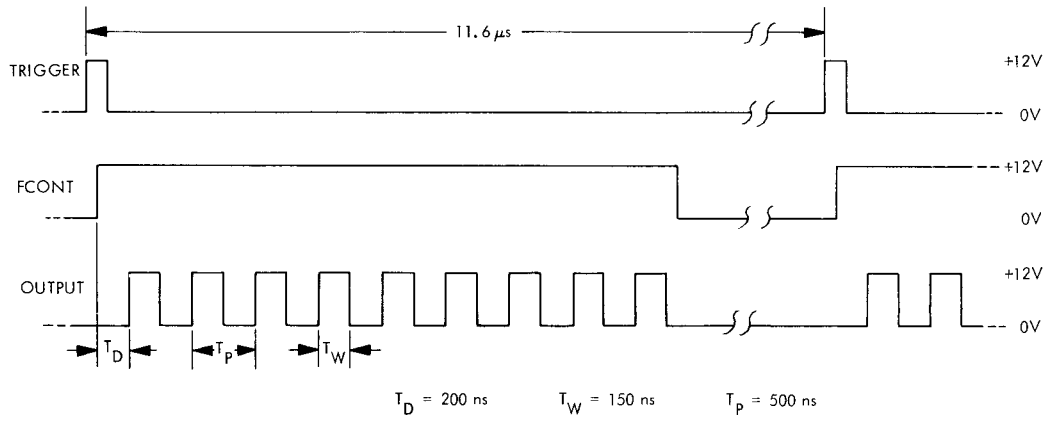

Fig. 4. Clock generator timing diagram

The system clock generator has been changed to a new design with more easily adjustable repetition rate and pulse width and improved independence of active component parameter variations. Figures 3 and 4 show the circuit and the timing diagram for the new clock generator. A trigger pulse, in synchronism with the incoming symbol frequency, sets control flip-flop FCONT, causing the generator to start outputting clock pulses after an initial delay T_D. After nine clock pulses, FCONT is reset by an external counter (not shown), thus terminating the clock sequence and making the generator ready to receive the next trigger. The value of C1 determines the delay T_D; the repetition rate $1/T_P$ and the pulse width T_W can be adjusted by means of R8 and R16, respectively.

D. Software Teletype Output Routines,

P. H. Schottler

1. Introduction

One of the requirements on the HRT software package is that it provides real-time information concerning the status of the HRT system both to the local station and to the Space Flight Operations Facility (SFOF). This dual requirement is fulfilled by using one of the teletype channels which interfaces with the telemetry and command processor (TCP) communications buffer. The local output is provided by a teletypewriter located at the station, and the output to the SFOF is provided over the teletype link connecting the station with the SFOF. The teletype output, together with the data output on magnetic tape, comprises the permanent record of the HRT system. The software routines which provide for teletype channel output are briefly described in this article.

2. Teletype Output

The teletype output takes two different forms. One form consists of alert messages which provide information about the current status of various components of the HRT system. The alert messages are intended primarily for use by the TCP operator at the local station. Typical alert messages provide information about the current lock status of the carrier and subcarrier loops, about the readiness of the magnetic tape units for data recording, and about mode transitions which occur as a result of word loop loss-of-lock. The alert message output is coded in order to minimize the time required to output the alert. A message consists of a time tag followed by a three-digit number, the first digit of which specifies the mode that the program is in (0, 1, 2, or 3), and two digits which specify the message number. A table lookup provides the operator with the message content and specifies what action, if any, is required.

The second form of teletype output consists of an estimate of the ratio of signal energy per information bit to noise spectral density (ST_B/N_0) in dB. This output provides a measure of the overall performance of the HRT system and is intended for use primarily by SFOF personnel to evaluate spacecraft performance. The estimate output consists of a time tag followed by a six-digit number (three places to either side of the decimal point and preceded by an algebraic sign) and is read directly in dB.

3. Teletype Routines

Five software routines participate in the output of teletype messages. They are teletype routines A, B, and C (TTRA, TTRB, and TTRC) shown in Figs. 5, 6, and 7, respectively, and teletype interrupt routines A and B (TIRA and TIRB) shown in Figs. 8a and 8b, respectively.

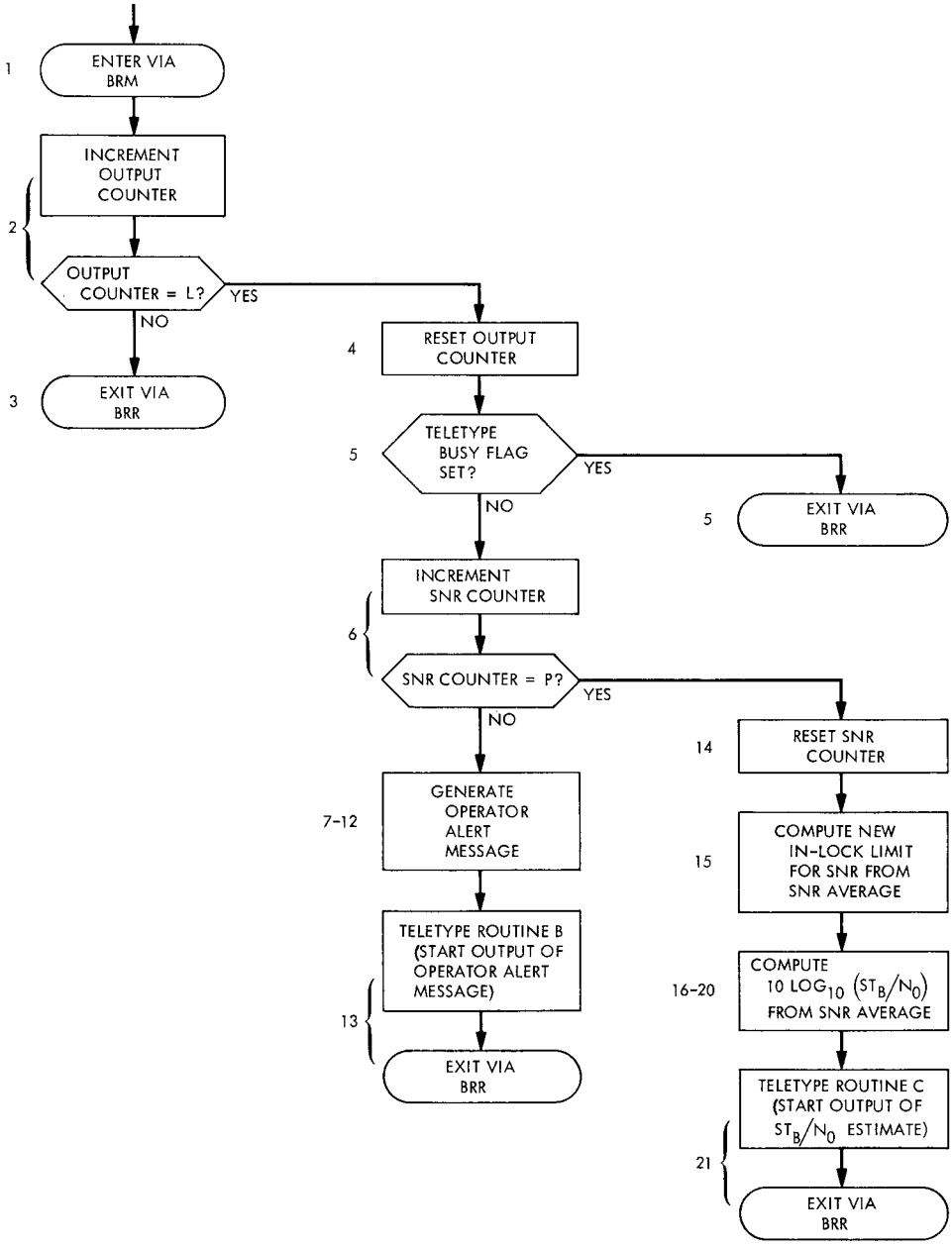

BRM MARK PLACE AND BRANCH
BRR RETURN BRANCH
SNR SIGNAL-TO-NOISE RATIO

Fig. 5. Teletype routine A (TTRA)

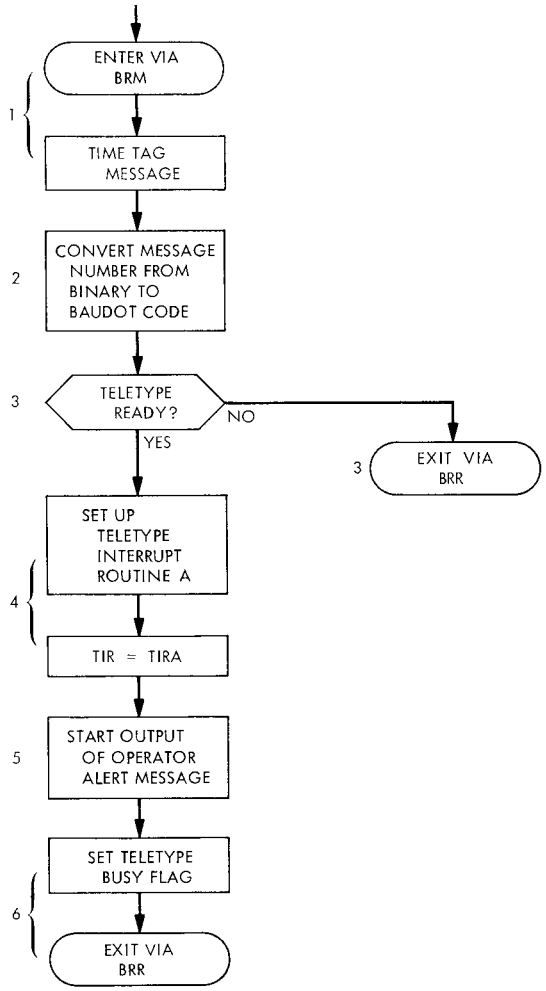

Fig. 6. Teletype routine B (TTRB)

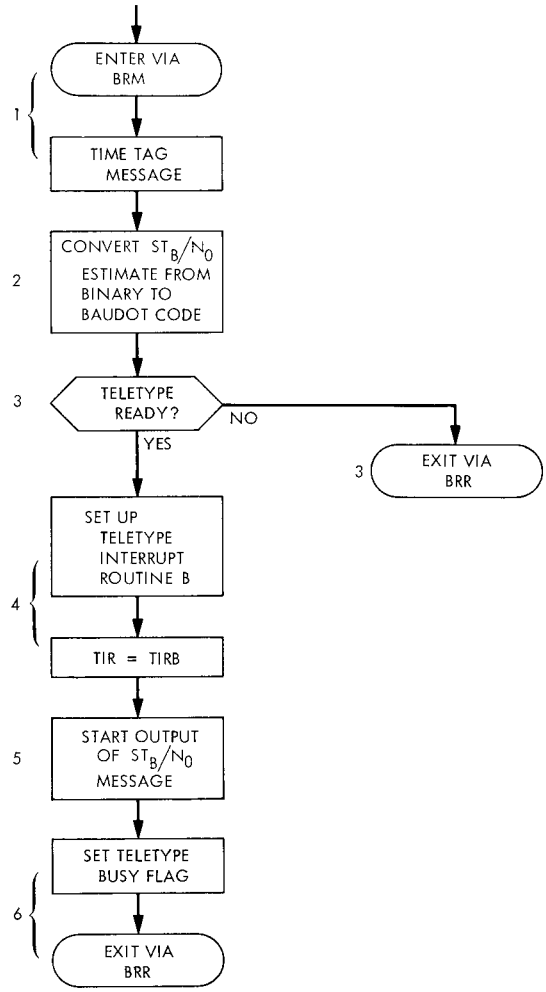

Fig. 7. Teletype routine C (TTRC)

Routine TTRA appears as block 33 of the data processing routine of mode 3 (SPS 37-48, Vol. II, p. 105, Fig. 16). Routines TTRA, TTRB, and TTRC are coded as subroutines, and entry is by means of a "mark place and branch" instruction.

Routines TTRA, TTRB, and TIRA handle the output of operator alert messages. After every group of L data records ($L = 20$) is written on magnetic tape, a status check of the various components of the HRT system is made in TTRA and the message number which corresponds to the current status of the system is generated. The program then enters routine TTRB where a time tag is added, the entire message converted from binary to five-level Baudot code, and the message output started. Control of the message output then passes to teletype interrupt routine TIRA. After each Baudot character is transmitted, a "teletype transmit end of word" interrupt occurs and the program enters routine TIRA where the next character is loaded into the channel. When the final character has been transmitted, the channel disconnects. During the time that the teletype channel is in the process of transmitting a message, the teletype busy flag is set. The flag is reset when the message output is complete. The program can test the teletype busy flag to determine when a new transmission can be started.

The "teletype transmit end of word" interrupt is a patchable 200-level interrupt in the TCP. Using a teletype channel rather than the TCP console typewriter to provide status information at the local station thus has the added advantage, as far as real-time operation is concerned, that the teletype channel is a low priority device whereas the console typewriter, which is on a noninterlaced buffer, is a high priority device (interrupt level 31).

Routines TTRA, TTRC, and TIRB handle the output of ST_B/N_0 estimates. After every group of $L \cdot P$ data

(a) TIRA

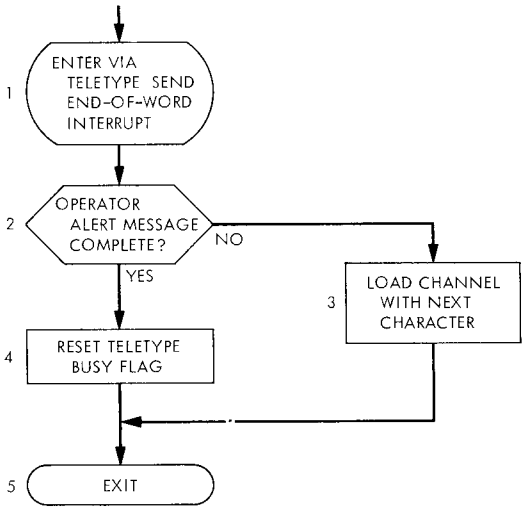

(b) TIRB

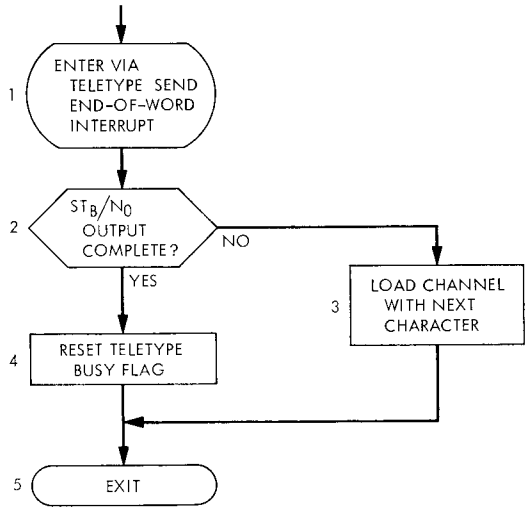

Fig. 8. Teletype interrupt routine A (TIRA) and B (TIRB)

records ($P = 5$) is written on magnetic tape, the quantity $10\log_{10}(ST_B/N_0)$ is computed in TTRA. The value of ST_B/N_0 used in this calculation is an average of ST_B/N_0 over the immediately preceding 100 data records. This average is computed in block 14 of the data processing routine of mode 3 (SPS 37-48, Vol. II, p. 105, Fig. 16). After the quantity $10\log_{10}(ST_B/N_0)$ is computed in TTRA, the program enters routine TTRC where a time tag is added, the entire message is converted from binary to Baudot code, and the message output is started. Control of the message output then passes to teletype interrupt routine TIRB.

The $\log_{10}$ calculation in TTRA makes use of straight-line approximations to the $\log_2$ function over three intervals of abscissa, the result being then converted to $\log_{10}$. The straight-line approximations are obtained by minimization of the mean-square error

$$\overline{\epsilon^2} = \int_a^b [\log_2 x - (ax + b)]^2\, dx \qquad 0.5 \leq a < b \leq 1.0$$

over each of the three intervals. The intervals are taken to be [0.5, 0.65], [0.65, 0.8], and [0.8, 1.0]. The absolute error in the calculation of $10\log_{10}(ST_B/N_0)$ does not exceed $8 \cdot 10^{-3}$. The standard Scientific Data Systems programmed operator for $\log x$ is not used because execution of the programmed operator takes too much time, and also because the algorithm contains a divide instruction which is non-interruptable for 28 memory cycles. A worst-case timing analysis of the program shows that this divide instruction could cause a data interrupt to be missed.

E. System Verification Tests, *R. W. Burt*

During July 1968, a series of system tests was performed using field set 1 at the compatibility test area. The measurement techniques discussed in previous SPS articles were used to determine the performance measurement of word error rate of the demodulated telemetry as a function of the RF input signal-to-noise ratio (ST_B/N_0).

Results were compiled two or three points at a time on July 9, 11, 12, 17, 18 and 19. A composite of the test results is shown in Fig. 9. Average degradation for the data is 0.47 dB, a degradation slightly worse than the high-rate telemetry design goal of 0.44 dB. Note that performance consistency was demonstrated over a period of six different days.

F. Effect of Variation in Subcarrier Loop Parameters on Telemetry Subcarrier Demodulator Performance, *M. H. Brockman*

1. Introduction

Theoretical performance characteristics for the telemetry subcarrier demodulator, which are applicable to a wide range of data rates for both uncoded and coded binary phase-shift-keyed telemetry, were presented in SPS 37-52, Vol. II, pp. 127–143. This article presents the effects of variation in the subcarrier tracking loop parameters on the basic performance characteristics of the telemetry subcarrier demodulator.

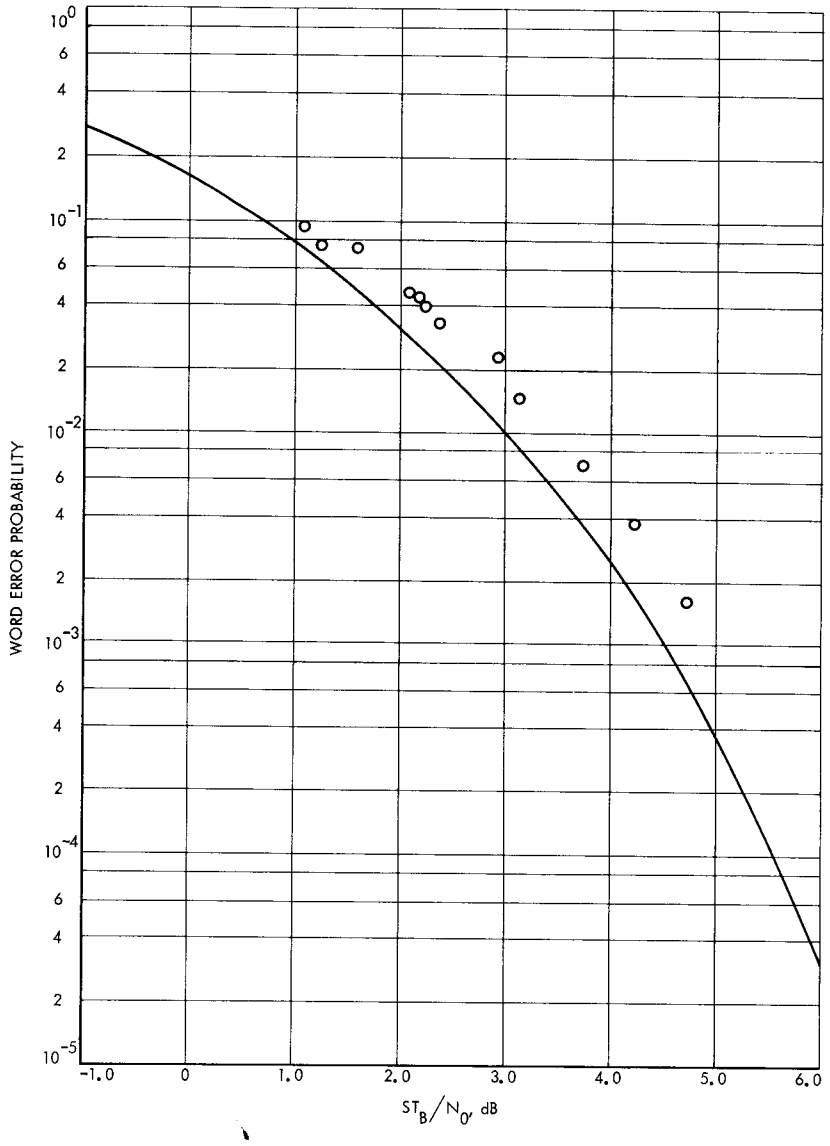

Fig. 9. High-rate telemetry test data

2. Subcarrier Tracking Loop Design and Telemetry Demodulator Performance

As developed in SPS 37-52, Vol. II, the performance of the telemetry subcarrier tracking loop is uniquely related to the signal-to-noise spectral density parameter $(\alpha')^2 \times S/N_0$ in the tracking loop predetection filter F_{A_2} for any signal level, telemetry data rate, and coding scheme within the capabilities of the DSIF S-band system. The factor α' represents the data suppression factor (SPS 37-46, Vol. III, pp. 189–204). The nominal noise bandwidth of the predetection filter F_{A_2} is 500 Hz, while the nominal design point parameters for the subcarrier tracking loop (which are contained in SPS 37-52, Vol. II) are presented in Table 1 for reference.

The following variations relative to the nominal (nom) design point parameters are applied herein to the theoretical expressions presented in SPS 37-52, Vol. II:

$$\frac{\alpha_{SL_0}}{\text{nom } \alpha_{SL_0}} = 0.91 \text{ to } 1.12$$

$$\frac{G_0}{\text{nom } G_0} = 0.70 \text{ to } 1.35$$

$$\frac{\tau_1}{\text{nom } \tau_1} \text{ and } \frac{\tau_2}{\text{nom } \tau_2} = 0.95 \text{ to } 1.05.$$

Table 1. Subcarrier loop design point parameters

Design point noise bandwidth, Hz	$(\alpha_0')^2 \times S/N_0$, dB	Soft bandpass limiter			G_0, 1/s	r_0', ratio	τ_1, s	τ_2, s
		α_{SL_0} ratio	ν ratio	Γ_{SL} ratio				
0.03	+1.7	0.0244	0.50	1.16	10	2.0	12,500	50
0.375	+9.7	0.0611	0.50	1.15	250	2.0	3000	4
1.50	+15.7	0.122	0.50	1.12	500	2.0	250	1

It should be pointed out that a variation in G_0 from 0.70 to 1.35 of nominal accommodates the following tolerances:

F_{A_2} noise bandwidth	500 ±100 Hz
Detector slope	0.9 to 1.1 of nominal
Voltage-controlled oscillator sensitivity	0.9 to 1.1 of nominal

plus a change in phase shift through the filter F_{A_2} and the soft bandpass limiter of 15 deg from design point to strong signals.

The effect of the variation in subcarrier loop design point parameters on two-sided closed-loop noise bandwidth BW_{SCL} is shown in Fig. 10 as a function of the signal-to-noise spectral density parameter $(\alpha')^2 \times S/N_0$ from equipment design point to strong signal levels for

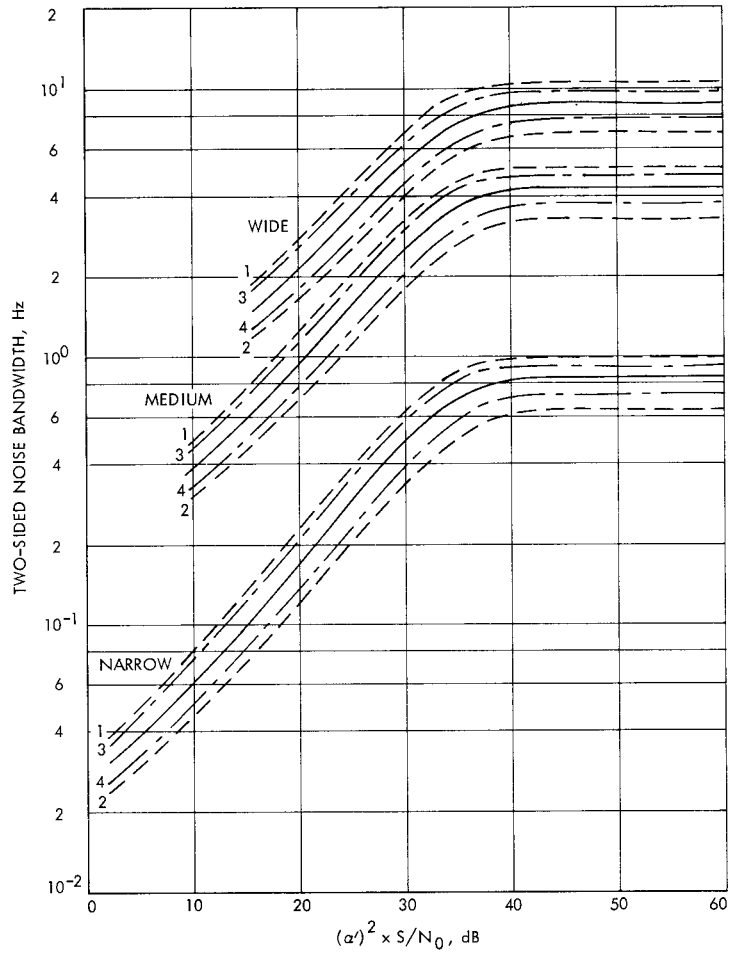

Fig. 10. Telemetry subcarrier demodulator two-sided closed-loop noise bandwidth vs predetection signal-to-noise spectral density ratio parameter

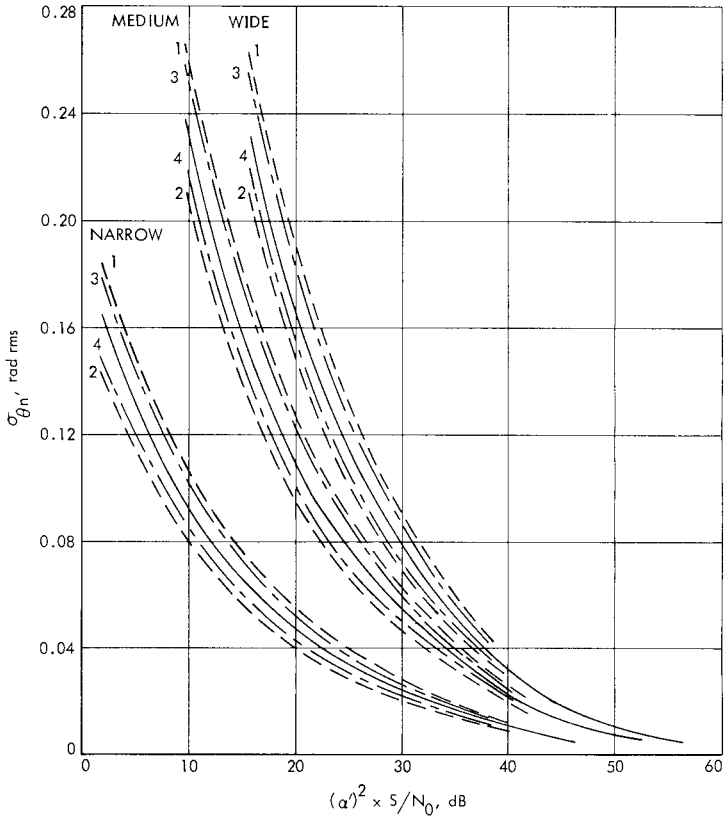

Fig. 11. Telemetry subcarrier demodulator rms phase noise error vs predetection signal-to-noise spectral density ratio parameter

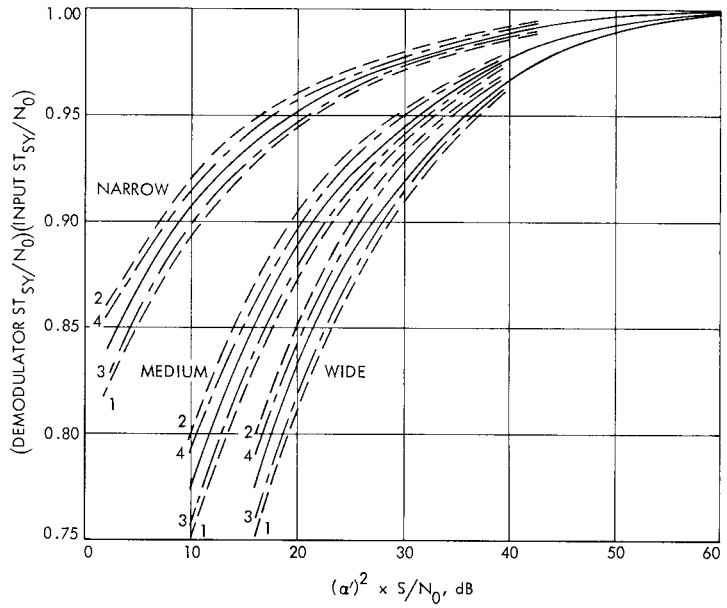

Fig. 12. Demodulated ST_{SY}/N_0 vs telemetry demodulator predetection signal-to-noise spectral density ratio parameter (subcarrier loop noise bandwidth: narrow, medium, wide)

the three bandwidths listed in Table 1. Following is the legend for Figs. 10–12.

————		Nominal
— — — —	1	G_0 = 1.35 nom, τ_1 and τ_2 = 0.95 nom
	2	G_0 = 0.70 nom, τ_1 and τ_2 = 1.05 nom
—.—.—.	3	G_0 = 1.25 nom, τ_1 and τ_2 = 0.95 nom
	4	G_0 = 0.80 nom, τ_1 and τ_2 = 1.05 nom

The resulting effect of design point parameter variation on the subcarrier tracking loop rms phase noise error $\sigma_{\theta n}$ is shown in Fig. 11 as a function of $(\alpha')^2 \times S/N_0$ for the three bandwidth designs listed in Table 1. The $\sigma_{\theta n}$ characteristics in Fig. 11 are applicable to any probability of data symbol stream switching and for any ratio of τ_D/τ_{SY} selected (SPS 37-52, Vol. II).

Finally, the effect of design point parameter variations on ratio of demodulated ST_{SY}/N_0 to input ST_{SY}/N_0 (demodulation efficiency) with zero phase error due to doppler frequency shift/rate is shown in Fig. 12 as a function of $(\alpha')^2 \times S/N_0$ for the three bandwidth designs listed in Table 1. It is interesting to note the following: With variation of G_0 from 0.70 to 1.35 of nominal plus variation of τ_1 and τ_2 from 1.05 to 0.95 of nominal, the resulting variation in demodulation efficiency at equipment design point is ± 0.020, ± 0.025, and ± 0.025 for the three bandwidth designs (Fig. 12).

Use of the performance characteristics shown in Figs. 10 through 12 is presented in SPS 37-52, Vol. II by application to *Mariner* Mars 1969.